Geant4 studies of the CNAO facility system for hadrontherapy treatment of uveal melanomas

2014 J. Phys.: Conf. Ser. 513 022028

(http://iopscience.iop.org/1742-6596/513/2/022028)

Journal of Physics: Conference Series **513** (2014) 022028 doi:10.1088/1742-6596/513/2/022028

Geant4 studies of the CNAO facility system for hadrontherapy treatment of uveal melanomas

A Rimoldi[1,2], P Piersimoni[1,2,3], M Pirola[1] and C Riccardi[1]

[1] Department of Physics, University of Pavia, via Bassi 6, 27100 Pavia, Italy
[2] INFN Pavia, via Bassi 6, 27100 Pavia, Italy
[3] Fondazione CNAO, strada privata Campeggi, 27100 Pavia, Italy

E-mail: Adele.Rimoldi@cern.ch, pierluigi.piersimoni@pv.infn.it

Abstract. The Italian National Centre of Hadrontherapy for Cancer Treatment (CNAO – Centro Nazionale di Adroterapia Oncologica) in Pavia, Italy, has started the treatment of selected cancers with the first patients in late 2011. In the coming months at CNAO plans are to activate a new dedicated treatment line for irradiation of uveal melanomas using the available active beam scan. The beam characteristics and the experimental setup should be tuned in order to reach the necessary precision required for such treatments. Collaboration between CNAO foundation, University of Pavia and INFN has started in 2011 to study the feasibility of these specialised treatments by implementing a MC simulation of the transport beam line and comparing the obtained simulation results with measurements at CNAO. The goal is to optimise an eye-dedicated transport beam line and to find the best conditions for ocular melanoma irradiations. This paper describes the Geant4 toolkit simulation of the CNAO setup as well as a modelised human eye with a tumour inside. The Geant4 application could be also used to test possible treatment planning systems. Simulation results illustrate the possibility to adapt the CNAO standard transport beam line by optimising the position of the isocentre and the addition of some passive elements to better shape the beam for this dedicated study.

1. Introduction

The hadrontherapy is an advanced radiotherapy technique which allows to deliver high dose to the target volume while sparing the healthy nearby tissue, thanks to the so-called "Bragg peak", generated by hadrons penetrating matter (Schardt *et al.*, 2010). The new Italian centre for oncological hadrontherapy (CNAO - *Centro Nazionale di Adroterapia Oncologica*) was opened in Pavia in early 2010. The CNAO facility is a synchrotron based medical centre where it is possible to treat deep seated big tumours with proton or carbon ion beams accelerated at very high energy (Amaldi, 2001; Pullia, 2008; Rossi, 2011). CNAO is designed for a fully active dose distribution system (Giordanengo *et al.*, 2010), the active scanning method.

One of the most successful fields of application of hadrontherapy (in particular protontherapy) is the treatment of uveal melanoma, a small but aggressive tumour growing inside of the eye (Egger *et al.*, 2001, 2003; Gragoudas *et al.*, 1977).

In the first phase of the CNAO activity an ocular dedicated beam line was not activated, but in the future one of the three treatment rooms available will be adapted and made suitable for ocular therapy.

The aim of the work reported in this paper is the implementation of a Monte Carlo simulation of

the CNAO transport beam line in order to check the possibility to make the CNAO experimental setup suitable for ocular treatments.

2. The Geant4 application

The core of this work is the implementation of a new hadrontherapy application in Geant4 (Agostinelli *et al.*, 2003; Allison et al., 2006), starting from the "advanced/hadrontherapy" example of the Geant4 distribution, and customising it with the necessary changes needed to simulate the standard CNAO transport beam line and a beam with the same characteristic of the CNAO proton beam. The Geant4 version used in this application is Geant4.9.5 patch01.

2.1. Geometry implementation

The simulated transport beam line is shown in figure 1(a). The elements are, respectively from the left hand side to right hand side: the vacuum beam pipe sealed by a thin carbon shutter called the exit-window, a fixed structure, the "nozzle", in which two beam monitoring chambers Box1 and Box2 are embedded, and the point where the patient is positioned, called the *isocentre*. Inside the nozzle frame some passive elements, such as ripple filters or range shifters, can be inserted if needed.

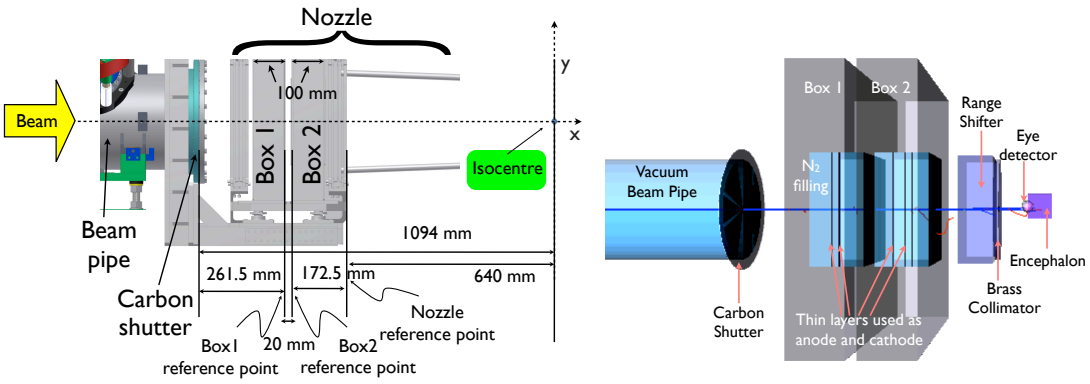

Figure 1. Schematisation of the CNAO beam line (a) and three-dimensional view of the simulated beam line in the Geant4 implementation (b).

The simulation frame of reference was chosen in order to have the X direction parallel to the beam propagation direction. The simulated geometry consists of all the elements described above positioned in a big air mother volume ($14 \times 14 \times 14$ m^3). Figure 1(b) shows the entire simulated beam line, including some passive elements (range shifter and collimator) and the eye-detector, described in detail in the next sections.

2.2. Particle generation and physical processes

Particle generation is done using the `G4VUserPrimaryGeneratorAction` class, opportunely modified for the simulation purpose. Both geometrical (the detector to be used, passive elements along the line etc.) and beam parameters (primary particle, its incident energy or momentum or position etc.) can be set. All these options can be set with no need of recompilation of the source code.

The beam can be fired in four different modalities, each one of them has its counterpart in the real CNAO setup: point-like, bi-dimensional scan with horizontal and vertical beam deflection

(Y and Z axes), energy variation for scans in the beam direction (X axis), three dimensional scan (Y, Z, energy) combining the two previous modalities.
The beam is generated with an energetic spread of about 0.15% corresponding to a relative momentum $\Delta p/p$ in the order of 10^{-4} and a Gaussian shape of the Y and Z profiles with a FWHM varying from 4 mm to 10 mm, inversely depending on the nominal particle's energy. These parameters are set in agreement to the CNAO synchrotron features (Pullia, 2008; Rossi, 2011).
In this implementation the physics list adopted is the same used in the "advanced/hadrontherapy" example of the Geant4 distribution. Electromagnetic, hadronic elastic and hadronic inelastic models available in Geant4 are therefore activated.

2.3. The eye-detector

One of the most amazing features of the Geant4 application described is the implementation of a detector faithfully reproducing a human eye, called the *eye-detector*. The first step in building the eye-detector was to analyse all the eye components and to assign to each of them a simpler geometrical shape to be implemented in Geant4. In figure 2(a) a drawing of a human eye and in figure 2(b) the simplified eye design adopted in this application are shown. The design of the eye model is based on studies on anatomy atlas (Netter, 2011; Standring, 2008).

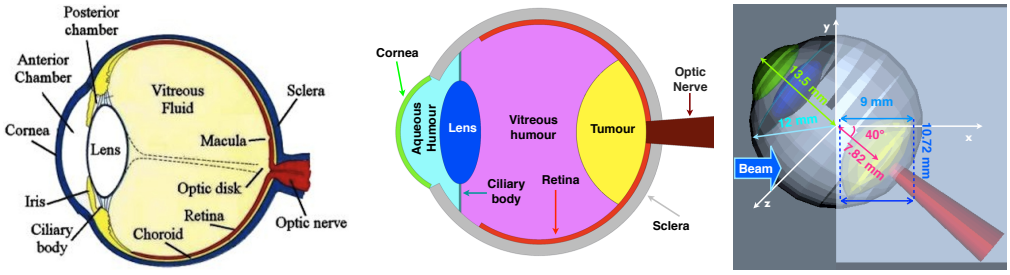

(a) (b) (c)

Figure 2. a), b) Comparison between a real human eye (a) and the simplified design used for the Geant4 implementation (b). c) Side view of the eye-detector implemented in the Geant4 simulation when rotated up by 40° for irradiation purposes.

All the eye components and a tumour, at the bottom of the eye, were implemented in the simulation. In figure 2(c) a side view of the simulated eye is presented. All the eye components are defined inside an "eye-world volume" which in turn is positioned inside the general world volume. This choice makes possible to rotate or translate the entire simulated eye just by moving the "eye-world volume", letting all the eye components maintain their mutual positions. Moreover the eye components are parameterised as a function of the sclera radius, so that changing it the whole eye is re-scaled. The sclera radius is changeable without need of recompilation.
For the eye components material implementation a two steps approach was used. Firstly a list of custom materials was created to reproduce all the chemicals present in a human eye. Then these starting materials were used in association, by the `AddMaterial` method, to form the final material for each eye component, to which a specific density is assigned. Each eye element is sensitive in the Geant4 simulation and separate hit collections, one for each of them, can be created in order to evaluate the dose deposition on the different tissues.

3. Validation of the Geant4 application

The simulation design described was validated against experimental data measured at CNAO. Experimental data used in this section are courtesy of Ciocca and Molinelli from CNAO Medical

Physics unit.
The beam FWHM was measured along the simulated beam line, at 4 different beam nominal energies: 81.56 MeV, 100.51 MeV, 119.05 MeV and 148.8 MeV. In figure 3(a) a comparison between simulated data and CNAO measured data with relative uncertainties is shown. The five experimental points refer to different positions along the beam line: at the exit window (-1112.5 mm), after the monitoring chamber Box 2 (-673 mm), at an intermediate point upstream the isocentre (-350 mm), at the isocentre (0 mm) and at a position downstream the isocentre (500 mm). The experimental uncertainties were evaluated to be about 10%. Simulated data were produced with 2.5×10^5 events generated in 5 statistical independent runs. Uncertainties (included in the point markers) are evaluated as square root of unbiased sample variances. The simulated detector for these measurements was a thin (1 mm thick) air layer detector, positioned at the five different distances along the simulated beam line. Experimental data and simulation overlap within the experimental uncertainties, therefore the agreement between simulated and measured data can be considered to be good. The percentage depth-dose deposited in a water phantom by simulated beams with 4 different nominal beam energies was measured and the proton range (depth penetration in water) for each nominal beam energy was calculated. In figure 3(b) simulation plots and CNAO experimental data are compared and a good overlap is achieved.

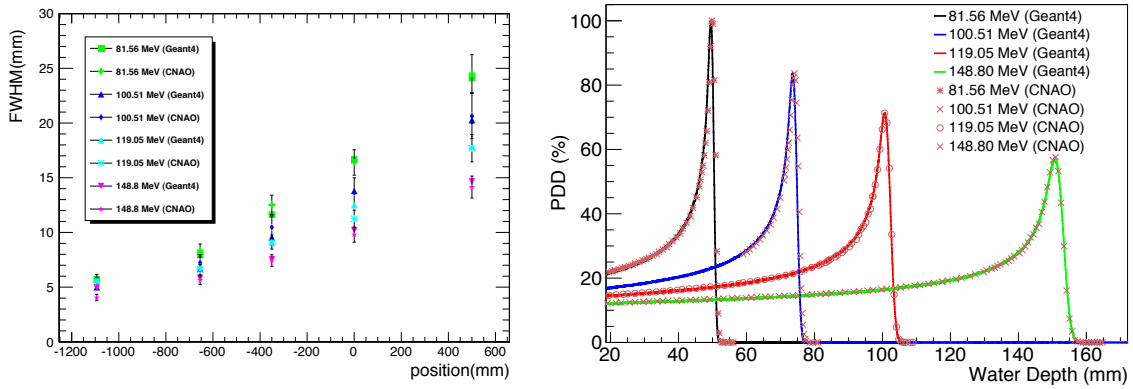

(a) (b)

Figure 3. a) Comparison between measured and simulated beam FWHM vs detector positions at four proton beam nominal energies. b) Percentage depth-dose deposited in a water phantom by proton beam with 4 different nominal energies. Curves are normalised at the dose deposited by the beam with lower energy (81.56 MeV).

Table 1. Proton range (depth penetration in water) for beam with 4 different nominal energies measured at CNAO and with the Geant4 simulation.

Beam nominal energy (MeV)	CNAO proton range (mm)	Geant4 proton range (mm)
81.56	50.00± 0.01	49.7±0.1
100.51	74.00± 0.01	73.7±0.1
119.05	101.00± 0.01	100.7±0.1
148.8	151.00± 0.01	150.7±0.1

The data were produced by simulating 2.5×10^5 events in 5 statistical independent runs. In table 1 the proton range measured in water at CNAO and the proton range measured with the simulated beam are reported. The discrepancy between simulation and experimental data is

lower than 1%, hence the agreement, again, can be considered good. The spatial resolution of the measured data is 0.01 mm, while in the simulation a read out geometry with a pixel of 0.05 mm was used. Uncertainties in table 1 account for both statistical and systematic errors.

4. Uniform dose deposition in the three dimensions

A PMMA range shifter was introduced in the transport beam line, in order to degrade the too high beam energy supplied by the CNAO synchrotron. For this reason a backwards shifting of the isocentre was needed, in order to minimise the beam broadening due to the introduction of the range shifter. The new isocentre is then defined at 11 cm from the end of the nozzle and the range shifter was positioned at a very close distance (6.5 cm) upstream the new isocentre. A uniform irradiation in the YZ plane was achieved in a large area, 40×40 mm^2, and then undesired lateral tails were cut with a brass collimator, 10 mm thick, with a 10 mm radius circular aperture, positioned at 5 cm upstream the isocentre. The simulated material for the brass collimator is an alloy of 61.5% of copper, 35.2% of zinc and 3.3% of lead (percentages in mass).
The mean values with the correspondent standard deviations and the lengths of the lateral penumbrae are reported in table 2 for both Y and Z profile, with or without the brass collimator. The values refer to the dose deposited in the central region (0.5 mm thick) of a thin water layer detector (1 mm thick) positioned at the isocentre. The addition of the brass collimator best focuses the dose deposition on the central area and halves the lateral penumbra in both the Y and Z profile.

Table 2. Dose average values and lateral penumbra for the Y and Z profile, obtained with a simulated irradiation on the transverse plane YZ.

	Mean Dose (mGy)		Fall-off 80-20% (mm)	
	Y	Z	Y	Z
No Collimator	4.48 ± 0.30	4.42 ± 0.28	7.25 ± 0.07	6.50 ± 0.07
Collimator In	7.75 ± 0.33	7.81 ± 0.30	4.00 ± 0.07	3.50 ± 0.07

4.1. Spread Out Bragg Peak

Because monochromatic proton beams are usually too narrow to cover spatial distributed treatment volumes, an extension in dose deposition in depth can be achieved by delivering not just one, but many Bragg peaks, each with a successively slightly different range (i.e., energy) and not all equally weighted (Goitein, 2008). The distal region of near-constant high dose is referred to as the "spread-out Bragg peak". An algorithm was implemented to calculate the set of correct weights necessary to obtain a SOBP and a simulated SOBP was produced inside a water cube detector ($25 \times 25 \times 25$ mm ^{3}) positioned at the new isocentre. The obtained SOBP (figure 4) inside of the water cube resulted to have a width of 18.10 ± 0.02 mm, extending from -8.9 mm upstream the new isocentre to 9.2 mm downstream the new isocentre. The peak/entrance ratio resulted 80% and the distal falloff of dose from 80% to 20% (the typical descriptor of penumbra) is 1.3 ± 0.02 mm. In the flat region the dose resulted fitted by a Gaussian distribution centred in 13.27 mGy and with a standard deviation of 0.20 mGy, with a uniformity of 1.5% The number of simulated events is $\sim 10^4$.

5. A simulated eye irradiation

After the studies of the beam shaping described in the previous section, an irradiation of the eye-detector was simulated, by performing a lateral beam scan, adding a 41 mm thick range shifter (65 mm upstream the isocentre) and a brass collimator with an ellipsoidal aperture of 20 mm $\times$ 22 mm (50 mm upstream the isocentre). The eye-detector was rotated of an angle of 40° in the vertical direction, in order to misalign the tumour from healthy tissues in front of it (e.g.

cornea and lens). With the setup just described, the treatment uniformity on the tumour in the eye-detector was tested.

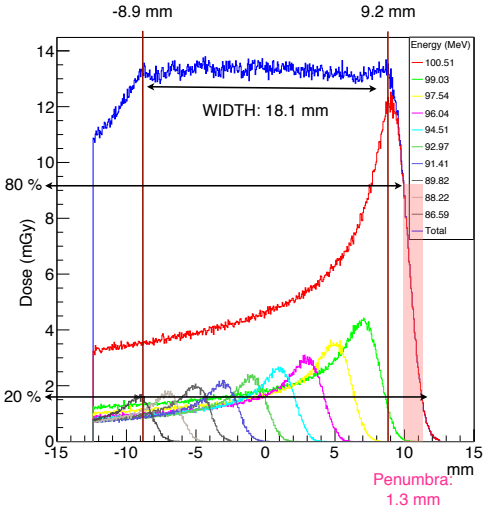

Figure 4. The SOBP (blue curve) obtained with the simulated beam line as a weighted sum of 10 energy distributions (coloured curves).

In figures 5(a) graphical representations of the dose distributions in two orthogonal planes (top and side projections) of the irradiated eye-detector with 3.6×10^6 events are shown. For a more quantitative description of the deposited dose in the eye-detector and for the evaluation of the ratio between the dose deposited in the tumour and the other eye components, comparative DVHs (Dose Volume Histograms) were built (figure 5(b)). A high statistics simulated sample (3.2×10^6 events) was used in order to have negligible statistics error. Looking at the DVH it is possible to see that 100% of the tumour volume results to have received a dose of 0.5 mGy, while the same dose is received by only the 40% of the vitreous humour volume. All the other eye components have an even lower dose deposition across their volume (from 40% to 20% or less). In particular in the optic nerve, the cornea and the lens, the most radiation sensitive sub components, 0.5 mGy have been deposited within 10% of their volume or less.

6. Conclusion

The work reported has allowed to evaluate the necessary changes to be done to the CNAO transport beam line in order to make it suitable for curing ocular melanomas. Tests have been performed by implementing a full Monte Carlo simulation using the Geant4 toolkit. The entire CNAO standard transport beam line was simulated, putting particular attention to implement each element, avoiding, when possible, any approximations. The eye-detector, one of the distinguish topics of the simulation, was realised after a deep study of the eye anatomy and chemical components. The validation of the simulation has been performed by comparing the simulated proton beam FWHM on the transverse plane and the proton range in water to the experimental data supplied by the CNAO staff. The standard transport beam line was adapted in the simulation in order to achieve a uniform three-dimensional dose deposition on the target volume inside of the implemented eye-detector, by shifting backwards the isocentre at 11 cm downstream the nozzle. The introduction of some passive elements (range shifter and collimator) led to a uniform irradiation on the target volume, achieving a good ratio between dose deposited on the tumour and on the other nearby healthy tissues. An eye treatment seems to be possible at the CNAO facility, by slightly modifying the transport beam line with the suggestions reported in this paper.

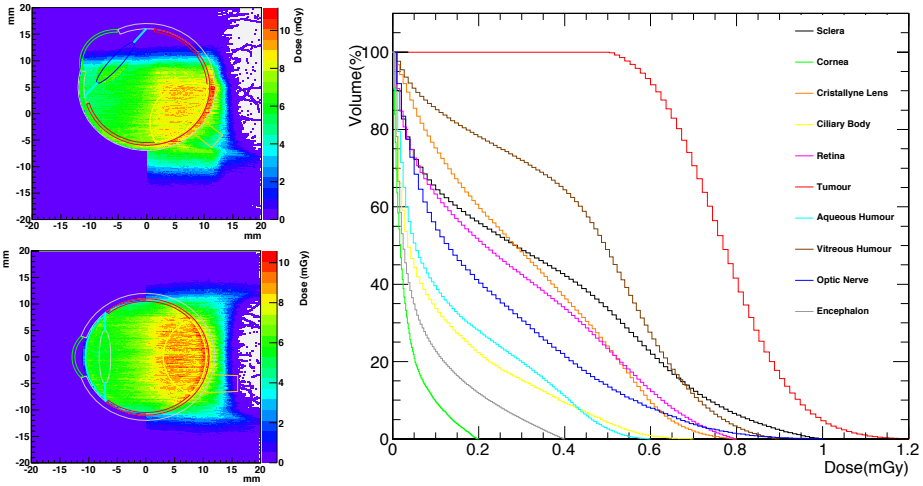

(a) (b)

Figure 5. a) Graphical representation of the dose distributions for an irradiation of the eye-detector. The tumour is represented by the yellow line in the right hand side of the eye. A side view (top) and a top view (bottom) of the irradiated eye-detector are shown. b) Comparative DVHs for simulated irradiation of the eye-detector.

References

Agostinelli S, Allison J, Amako K, Apostolakis J *et al.* 2003 Geant4 - A Simulation Toolkit *Nucl. Inst. & Meth. A* **506** 250-303

Allison J, Amako K, Apostolakis J *et al.* 2006 Geant4 developments and applications *Transaction on Nuclear Science* **53** 270-278

Amaldi U 2001 The Italian hadrontherapy project CNAO *Physica Medica* **XVII** (1)

Egger E, Schalenbourg A, Zografos L *et al.* 2001 Maximizing local tumor control and survival after proton beam radiotherapy of uveal melanoma, *Int J Radiat Oncol Biol Phys.* **51** 138-147

Egger E *et al.* 2003 Eye retention after proton beam radiotherapy for uveal melanoma Int *J Radiat. Oncol Biol Phys.* **55** 867-880

Giordanengo S *et al.* 2010 Performances of the scanning system for the CNAO center of oncological hadron therapy *Nucl. Inst. & Meth. A* **613** 317–322

Goitein M 2008 *Radiation Oncology: A Physicist's-Eye View* (NY: Springer)

Gragoudas E S, Goitein M, Koehler A M *et al.* 1977 Proton irradiation of small choroidal malignant melanomas *Am. J. Ophthalmol.* **83** 655–673

Netter F H 2011 *Atlas of Human Anatomy - Fifth Edition* (MO: Saunders-Elsevier)

Pullia M 2008 Status report on the Centro Nazionale di Adroterapia Oncologica (CNAO)*EPAC08, TUOCG02*

Rossi S 2011 The status of CNAO *Eur. Phys. J. Plus* **126** 78

Schardt D, Elsässer T and Schulz-Ertner D 2010 Heavy-ion tumor therapy: Physical and radiobiological benefits, *Reviews of modern physics* **82**, 383-425

Standring S, 2008 Gray's Anatomy 40th Edition (UK: Churchill Livingstone/Elsevier)